SHE RESEARCH AT RIKEN NISHINA CENTER*

H. Sakai, P. Brionnet

for the nSHE Research Group

RIKEN Nishina Center, Japan

Received 9 December 2023, accepted 29 January 2024, published online 24 April 2024

To synthesize a new superheavy element, $Z = 119$, the RIKEN Nishina Center (RNC) has upgraded the existing heavy-ion linac system (called RILAC) to the superconducting linear accelerator system (SRILAC) to enable a hot fusion reaction of $^{51}\mathrm{V} + ^{248}\mathrm{Cm}$. The upgraded project, called the 'SHE project', was completed in 2020. After the commissioning of SRILAC, the first step was to measure the Coulomb barrier distribution for the $^{51}\mathrm{V} + ^{248}\mathrm{Cm}$ system in order to deduce the optimal bombarding energy of the $^{51}\mathrm{V}$ beam. The measurement of the synthesis of $Z = 119$ was then started and is still going. The side-collision effect due to nuclear deformation should play an important role in maximising the synthesis cross section. Since $^{159}\mathrm{Tb}$ and $^{248}\mathrm{Cm}$ have a similar amount of deformation ($\beta \sim 0.28$), the $^{51}\mathrm{V} + ^{159}\mathrm{Tb}$ reaction was used to study the deformation effect. The $^{51}\mathrm{V} + ^{159}\mathrm{Tb}$ reaction has large fusion reaction cross sections and, therefore, the Coulomb barrier distribution as well as the evaporation residues for the xn, pxn, and αxn exit channels could be measured. The evaporation residue cross sections are compared with those of the simple statistical decay model calculation.

DOI:10.5506/APhysPolBSupp.17.3-A21

1. Overview of the nSHE project and its present status

The SHE project consisted of upgrading the RILAC accelerator by partially replacing the RIKEN superconducting linear accelerator (SRILAC) to increase the final beam energy from 5.5 MeV/u to 6.5 MeV/u, and the construction of a new Superconducting Electron Cyclotron Resonance Ion Source (SC-ECRIS) operating at a higher RF frequency to increase the beam current. The new gas-filled recoil ion separator GARIS-III, suitable for hot fusion reaction products, was designed and constructed. The upgraded SHE project and its commissioning results were described in detail in Ref. [1].

* Presented at the XXXVII Mazurian Lakes Conference on Physics, Piaski, Poland, 3–9 September, 2023.

The barrier distribution for the entrance channel of the ^{51}V+^{248}Cm system was deduced by measuring the quasi-elastic (EQ) backscattering cross sections σ_{QE} at $\theta = 180°$ with GARIS-III when SRILAC was operational. The barrier distribution provided the mean Coulomb-barrier height as $B_0 = 225.6 \pm 0.2$ MeV for the ^{51}V+^{248}Cm system.

It has been pointed out that the side-collision configuration (compact configuration) between the projectile and the deformed target nucleus is important to realize the maximum evaporation residue (ER) cross section. The side-collision effect (ΔE_{side}) can be estimated using coupled-channel calculations. For the ^{51}V+^{248}Cm system, it was found to be $\Delta E_{\mathrm{side}} = 7.4$ MeV. Taking another small effect of 1.8 MeV into account, the final bombarding energy of ^{51}V was chosen to be E_{beam}(optimal) = 234.8 MeV ($B_0 + \Delta E_{\mathrm{side}} + 1.8$ MeV), corresponding to $E^*\left[^{299}119\right] = 40.3$ MeV. The results are reported by Tanaka *et al.* in Ref. [2].

Thus, the experimental conditions for the synthesis of $Z = 119$ by the ^{51}V+^{248}Cm reaction were established and the $Z = 119$ synthesis measurement started in 2020.

The SRILAC was able to provide sufficient ^{51}V beam intensity of a few pμA for the measurement. The target prepared by electrodeposition consists of $^{248}Cm_2O_3$ and a backing film.

A serious concern is the lifetime of the target. High-intensity beams quickly damage the backing material. We are still testing various backing materials that will last longer and withstand substantial energy losses, equivalent to 10–30 W heat loss in the target+backing materials depending on the beam intensities 1–3 pμA [1].

Since both the SHE project and the measurement of the barrier distribution to derive the optimal beam energy have been described in detail elsewhere [1, 2], we will not repeat them. Instead, in the following sections we describe the recent measurement of the ^{51}V+^{159}Tb reaction to study fusion reaction mechanisms. The ^{51}V+^{159}Tb reaction is suitable because it has the advantage of much higher ER production rates (μb range).

2. Study on fusion reaction mechanisms

The ER cross section, σ_{ER}, is often described as a product of three steps, the capture cross section σ_{cap}, the fusion probability P_{fus}, and the survival probability P_{surv}. This model is essentially based on the classical mechanics, although each step heavily incorporates quantum mechanical predictions

$$\sigma_{\mathrm{ER}} = \sigma_{\mathrm{cap}} \times P_{\mathrm{fus}} \times P_{\mathrm{surv}} \,. \tag{1}$$

[1] 1 pμA is equal to 6.24×10^{12} particles/s.

Here, dependence on the angular momentum (ℓ), the collision energy in CM system ($E_{\rm CM}$), and the excitation energy of the compound nucleus (E^* or $U_{\rm CN}$) are suppressed for convenience.

To explore the fusion reaction mechanism, the ^{51}V+^{159}Tb reaction was studied with some emphasis on:

— Side-collision effect: Very little information is currently available. It is considered due to the deformation of the target nucleus, and it relates to $\sigma_{\rm cap}$. Note that the nuclear deformation of ^{159}Tb ($\beta_2 \sim 0.28$) is similar to that of ^{248}Cm.

— Statistical decay property: Almost no data are available for the measurement of the ERs for the xn, pxn, and αxn exit channels, simultaneously. The exit channel ER cross sections are directly related to $P_{\rm surv}$.

3. Measurement of ^{51}V+^{159}Tb reaction

Experimental conditions and procedure are described in Refs. [3, 4].

3.1. Quasi elastic cross section (σ_{QEL}), barrier distribution, B_0, and B_{side}

Figure 1 shows the Rutherford ratio R defined as $\sigma_{\rm QEL}/\sigma_{\rm Ruth}$ (top) and the barrier distribution $({\rm d}\sigma_{\rm QEL}/{\rm d}\sigma_{\rm Ruth})/{\rm d}E$ (bottom). The points (blue/dark grey and green/grey) are the measured data, and the curves are CCFULL calculations [5] with different input parameters. The $R = 0.5$ value provides B_0. The vertical arrows indicate the $B_0 = 164$ MeV and $B_{\rm side} = 172$ MeV values, respectively. The obtained $B_{\rm side}$ value is compared with the precise excitation function we simultaneously measured for this reaction.

3.2. Excitation function for ^{51}V+^{159}Tb for xn, pxn, and αxn exit channels

Figure 2 shows the measured cross section of the xn, pxn, and αxn exit channels for the ^{51}V+^{159}Tb $\rightarrow$ ^{210}Ra* reaction as a function of $E_{\rm CM}$.

The maximum cross sections for $\sigma^m_{\rm exp}$ for $3n$, $p3n$, and $\alpha 3n$ exit channels are 4.4 μb at $E^* = 40$ MeV, 33 μb at $E^* = 56$ MeV, and 54 μb at $E^* = 56$ MeV, respectively[2].

Surprisingly, there is no evidence for the side-collision effect. It is expected to have the maximum cross section for the $3n$ or $4n$ exit channel at $B_{\rm side}(= 172$ MeV). The reason for its disappearance needs to be understood.

[2] The acceptance of GARIS-III is reduced by the momentum kick associated with the α-particle emission, which reduces the efficiency of ER detection. Therefore, the value of $\sigma(\alpha 3n)$ is modified. Here we assume 50% transmission for simplicity. The original measured value given in Fig. 2 is 27 μb.

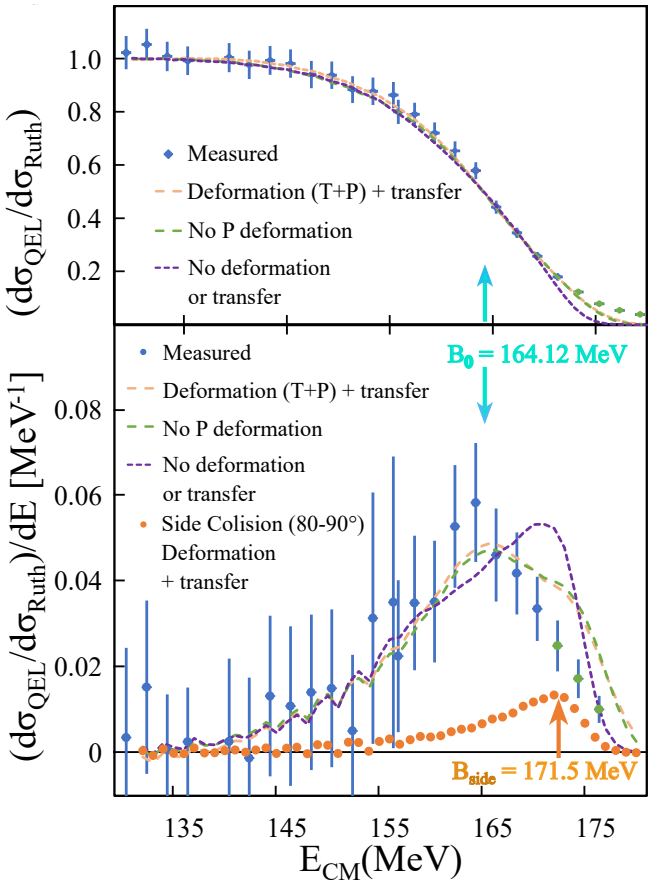

Fig. 1. (Colour on-line) Rutherford ratio R (top panel) and barrier distribution (bottom panel) of the ^{51}V+^{159}Tb reaction taken from Ref. [3].

Even more surprising is that the cross sections for the $p3n$ and $\alpha 3n$ charged-particle exit channels are larger by about an order of magnitude than those for the $3n$ exit channel, which has no Coulomb barrier. In the next section, we try to understand these phenomena in terms of the statistical decay model of the compound nucleus.

4. Statistical decay of the compound nucleus ^{210}Rd

It is very convenient to estimate the n, p, and α decays in terms of decay widths from the compound nucleus based on the simple statistical model assumption. The decay-width estimate is useful and convenient for making a quick qualitative guess. However, it should be remembered that this treatment is for an order estimate.

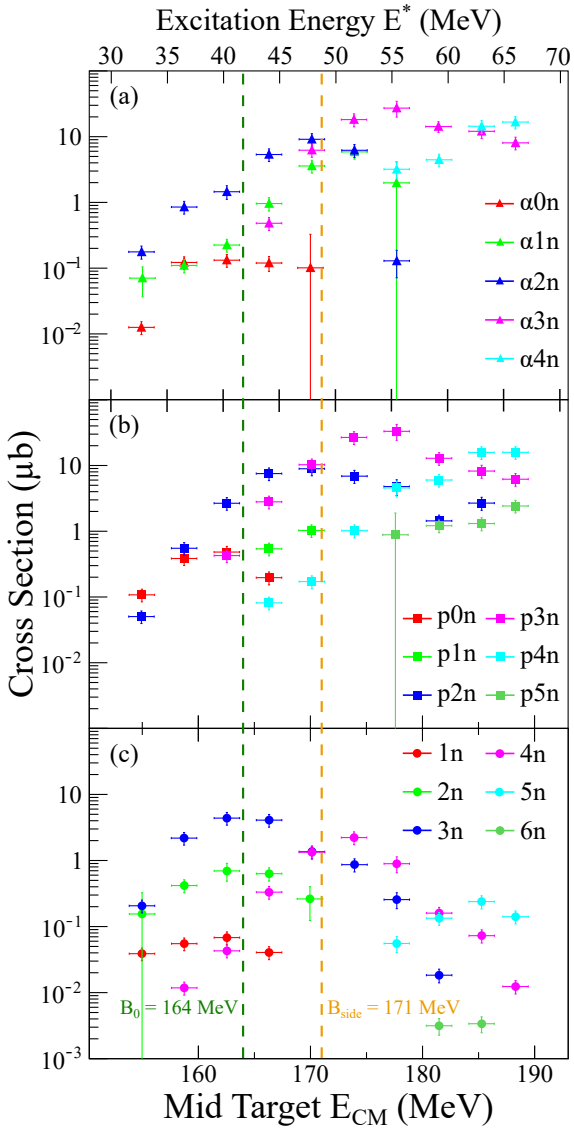

Fig. 2. (Colour on-line) Excitation function of the ^{51}V+^{159}Tb reaction: (a) αxn exit channel, (b) pxn exit channel, (c) xn exit channel. Vertical green/black (yellow/grey) dashed line indicates the $B_0 = 164$ MeV value ($B_{\rm side} = 171$ MeV value). Data are taken from Ref. [4].

It is assumed that the charged particles, the proton and the α, are emitted at first during the pxn and αxn decay processes (first chance decay).

The ratio of decay widths of competing decay particles can be estimated rather accurately

$$\frac{\Gamma_p}{\Gamma_n} \approx \frac{E^* - B_p}{E^* - B_n} \exp\left(\frac{B_n - B_p - V_{\rm C}^p}{T}\right), \tag{2}$$

$$\frac{\Gamma_\alpha}{\Gamma_n} \approx 2\frac{E^* + Q_\alpha}{E^* - B_n} \exp\left(\frac{B_n + Q_\alpha - V_{\rm C}^\alpha}{T}\right), \tag{3}$$

$$\frac{\Gamma_n}{\Gamma_{\rm f}} \propto \frac{A^{2/3}}{5.286\sqrt{a}} \frac{E^* - B_n}{\sqrt{E^* - B_{\rm f}}} \exp\left(\frac{B_{\rm f} - B_n}{T}\right), \tag{4}$$

where Γ_n, Γ_p, and Γ_α are the n-, p-, and α-decay widths, respectively. B_n, B_p, $B_\alpha(= -Q_\alpha)$ are the binding energies of neutron, proton, and α particle of compound nucleus, respectively and $B_{\rm f}$ is the fission barrier height. $V_{\rm C}^p$ and $V_{\rm C}^\alpha$ are the Coulomb barrier heights for protons and α particles, respectively. Equations (2)–(4) contain an extra prefactor before the exponent that improves typical ratio formulas from the statistical model [6]. These equations were derived by assuming Fermi gas level densities where a is a nuclear level-density parameter that is assumed to be independent of decay channels and excitation energy.

It is also assumed

$$T = T_n = T_p = T_\alpha = T_{\rm f}\,. \tag{5}$$

The angular momentum effects are also neglected. In some extreme cases, these assumptions become serious, but we expect that the order of magnitude would remain valid in the present analysis.

4.1. Decay-width estimate of $^{210}Ra^*$

4.1.1. Input parameters

Let us apply Eqs. (2)–(4) to extract $\Gamma_{n/p/\alpha}$ from an excited state of ^{210}Ra* at the excitation energies of $E^* = 37$ and 56 MeV.

The following values are used:

$$\begin{aligned}
B_n &= 9.5 \text{ MeV}, \\
B_p &= 3.1 \text{ MeV}, \\
B_\alpha &= -7.2 \text{ MeV} \quad (= -Q_\alpha), \\
B_{\rm f} &= 13.3 \text{ MeV} \quad \text{(See Ref. [7])}, \\
V_{\rm C}^p &= 8.32 \text{ MeV} \quad \text{(See Ref. [8])}, \\
V_{\rm C}^\alpha &= 18.6 \text{ MeV} \quad \text{(See Ref. [8])}.
\end{aligned}$$

The temperature in Eqs. (2)–(3) can be estimated using a

$$\begin{aligned} E^* &= aT^2\,, \\ \text{where} \quad a &= \frac{A}{14.61}\left(1+4\times A^{-1/3}\right) \quad \text{(See Ref. [9])} \\ &= 24\ \text{MeV}^{-1}\,. \end{aligned} \tag{6}$$

The temperatures of interest are

$$\begin{aligned} E^* &= 37\ \text{MeV} \rightarrow T = 1.24\ \text{MeV}\,, \\ &= 56\ \text{MeV} \rightarrow T = 1.53\ \text{MeV}\,. \end{aligned}$$

4.1.2. Ratio of widths and P^{Γ}_{surv}

The ratios at $E^* = 37$ MeV ($E^* = 56$ MeV) can be extracted using Eqs. (2)–(4) as

$$\frac{\Gamma_p}{\Gamma_n} = 0.26\ \ (0.33)\,, \tag{7}$$

$$\frac{\Gamma_\alpha}{\Gamma_n} = 0.70\ \ (0.93)\,, \tag{8}$$

$$\frac{\Gamma_n}{\Gamma_\text{f}} = 165\ \ (116) \rightarrow \frac{\Gamma_\text{f}}{\Gamma_n} = 0.006\ \ (0.009)\,. \tag{9}$$

These ratios can be expressed as

$$\Gamma_n : \Gamma_p : \Gamma_\alpha : \Gamma_\text{f} = 1.0\ (1.0) : 0.26\ (0.33) : 0.70\ (0.93) : 0.007\ (0.009)\,. \tag{10}$$

Since the fission decay due to the relatively high barrier is an order of magnitude smaller than the neutron decay, therefore, we will no longer consider the fission competition.

Let us define the branching ratio formula as

$$P^{\Gamma}_{\text{surv}} \overset{\text{def}}{\equiv} \Gamma_n : \Gamma_p : \Gamma_\alpha\,. \tag{11}$$

As expected from the lack of the Coulomb barrier, the neutron emission dominates, but not by much, only 3–4 times as much as the proton emission and is even comparable to the α emission.

4.1.3. Evaporation residue cross section, $\sigma^{\text{SM}}_{\text{ER}}$, from statistical model

Neglecting the effects of two (three) neutron emissions after the first chance decays by a proton, or an α particle, we can estimate the ER cross section, $\sigma^{\text{SM}}_{\text{ER}}$, at $E^* = 37$ (56) MeV if we can estimate σ_{cap} and P_{fus} in Eq. (1).

The Fusion-by-Diffusion (FBD) model [10] is often applied to estimate the ER cross section $\sigma_{\rm ER}$. Such a calculation provides the entrance channel cross section, $\sigma_{\rm cap}$. For the ^{51}V+^{159}Tb reaction, the $\sigma_{\rm cap}^{\rm FBD}$ value has been derived as ~ 45 (250) mb at $E^* = 37$ (56) MeV [6]. $P_{\rm fus} = 1.4 \times 10^{-3}$ is also assumed [6].

The branching ratio for the survival process is obtained by renormalizing the total decay width, $\Gamma^{\rm tot} = \Gamma_n + \Gamma_p + \Gamma_\alpha$, namely

$$\left\langle P_{\rm surv}^{\Gamma} \right\rangle \stackrel{\rm def}{\equiv} \frac{\Gamma_n}{\Gamma^{\rm tot}} : \frac{\Gamma_p}{\Gamma^{\rm tot}} : \frac{\Gamma_\alpha}{\Gamma^{\rm tot}} \begin{array}{l} = 0.51 : 0.13 : 0.36 \quad \text{at } E^* = 37 \text{ MeV}, \\ = 0.44 : 0.15 : 0.41 \quad \text{at } E^* = 56 \text{ MeV}. \end{array} \quad (12)$$

Thus, the ER cross section for the $xn/pxn/\alpha xn$ decay channels is expressed as

$$\sigma_{\rm ER}^{\rm SM}(xn/pxn/\alpha xn) = \sigma_{\rm cap}(E^*) \times P_{\rm fus} \left(= 1.4 \times 10^{-3}\right) \times \left\langle P_{\rm surv}^{\Gamma} \right\rangle . \quad (13)$$

4.2. Comparisons at $E^* = 37$ MeV

At $E^* = 37$ MeV, the dominant ERs are ^{207}Ra ($3n$), ^{207}Fr ($p2n$), and ^{204}Rn ($\alpha 2n$). A comparison between $\sigma_{\rm exp}$ and $\sigma_{\rm ER}^{\rm SM}$ values is presented in Table 1. Note that $E* = 37$ MeV is well below the Coulomb-barrier height, $B_0 = 40$ MeV, so the cross section is mainly due to the sub-barrier fusion reaction, which is essentially determined by the transmission of the Coulomb barrier.

Table 1. Cross sections for the ^{159}Tb(^{51}V, $3n/p2n/\alpha 2n$) reactions at 37 MeV excitation energy.

Channel	$3n$	$p2n$	$\alpha 2n$	
E^*	37 MeV	37 MeV	37 MeV	
$\sigma_{\rm exp}$ [μb]	2	0.55	1.6	Ref. [4]
$\sigma_{\rm ER}^{\rm SM}$ [μb]	7	2	5	$\sigma_{\rm cap} = 10$ mb, $\langle P_{\rm surv}^{\Gamma} \rangle$

Interestingly, the cross sections of the experimentally observed ER for the $3n$, $p2n$, and $\alpha 2n$ channels and their relative ratio seem to be well-estimated by the simple statistical model calculations within a factor of 3. Thus, the fusion reaction at the sub-barrier energy showed the expected statistical decay property.

4.3. Comparisons at $E^* = 56$ MeV

At $E^* = 56$ MeV, the dominant ERs are ^{206}Ra ($4n$), ^{206}Fr ($p3n$), and ^{203}Rn ($\alpha 3n$). A comparison between $\sigma_{\rm exp}$ and $\sigma_{\rm ER}^{\rm SM}$ values is presented in Table 2.

Table 2. Cross sections for the ^{159}Tb(^{51}V, $4n/p3n/\alpha 3n$) reactions at 56 MeV excitation energy.

Channel	$4n$	$p3n$	$\alpha 3n$	
E^*	56 MeV	56 MeV	56 MeV	
$\sigma_{\rm exp}$ [μb]	1.0	33	54	Ref. [4]
$\sigma_{\rm ER}^{\rm SM}$ [μb]	154	53	143	$\sigma_{\rm cap} = 250$ mb, $\langle P_{\rm surv}^{\Gamma} \rangle$

In the $\alpha 3n$ channel, $\sigma_{\rm exp}/\sigma_{\rm ER}^{\rm SM}$ is $\sim 1/3$, while in the $4n$ channel, this ratio amounts $\sim 1/150$ showing a clear reduction of more than two orders of magnitude. Thus, it is clear that the experimental value of the neutron $4n$ exit channel clearly shows a significant suppression compared to the charged-particle $\alpha 3n$ exit channel.

5. Final remarks

With the aim of synthesizing the new element $Z = 119$ via the ^{51}V $+^{248}$Cm hot fusion reaction, the SHE project was initiated in 2016 with the construction of the SRILAC, SC-ECRIS, and GARIS-III facilities at RNC. With the completion of the equipment, the commissioning of the whole facility started in 2020.

To determine the optimal bombarding energy, the barrier distribution for the ^{51}V+^{248}Cm entrance channel was deduced by measuring the quasi-elastic (EQ) scattering. The mean Coulomb-barrier height was estimated as $B_0 = 225.6 \pm 0.2$ MeV for the ^{51}V+^{248}Cm system. The side-collision effect was also estimated by the CCFULL calculation to be 7.4 MeV. The optimal bombarding energy was chosen to be $E_{\rm beam}$(optimal) = 234.8 MeV ($B_0 + \Delta E_{\rm side} + 1.8$ MeV), corresponding to E^* $\left[^{299}119\right] = 40.3$ MeV.

To study the side-collision effect and the entrance-channel effect, the barrier distribution as well as ERs for the ^{51}V+^{159}Tb reaction were measured simultaneously for the xn, pxn, and αxn exit channels, where the deformation parameter of ^{159}Tb is comparable to that of ^{248}Cm.

We were surprised to find no evidence for the side-collision effect in the xn channel of the ER data. We would like to understand the reason for this, as it could significantly affect the choice of the optimal collision energy

for the synthesis of the new $Z = 119$ element by the hot fusion reaction ^{51}V+^{248}Cm. The disappearance of the side-collision effects is under discussion with Hagino [5].

It was also a surprise to find in the ERs that the αxn exit channel dominates over the xn exit channel in the high-excitation region of $E^* \sim 45$ MeV. To understand this surprising feature, we performed simple statistical decay model calculations which give the decay widths for the xn, pxn, and αxn channels, *i.e.* the branching ratio $P_{\rm surv}$. At $E^* = 56$ MeV, the calculated ratio is $P_{\rm surv}(4n/\alpha 3n) = 0.41/0.44 \sim 1$, while the experimental branching ratio was $\sigma(4n)/\sigma(\alpha 3n) = 1/54 \sim 0.02$. It is clear that the $4n$ channel is suppressed by two orders of magnitude compared to the $\alpha 3n$ channel. As a reference to the simple statistical calculation, we compared the calculated result with the experimental value at $E^* = 37$ MeV, where the reaction is considered to be a sub-barrier fusion reaction. The result is $P_{\rm surv}(3n/\alpha 2n) = 7/5 \sim 1.4$, while the experimental branching ratio was $\sigma(3n)/\sigma(\alpha 2n) = 2/1.6 \sim 1.3$. It is interesting to note that the simple statistical model provides a good description of the fusion reaction at sub-barrier conditions. The data will be soon compared with detailed statistical decay model calculations performed by the Warsaw group using the fusion-by-diffusion (FBD) assumption [10].

At this point, it should be noted that the height of the fusion barrier plays an essential role, especially in the ^{51}V+^{248}Cm $\rightarrow^{299}$119 fusion process, where $B_{\rm f} \sim 6$–8 MeV. In contrast, for ^{51}V+^{159}Tb $\rightarrow^{210}$Rd, $B_{\rm f} = 13.7$ MeV and, therefore, it does not contribute to the decay process.

The original intention of the ^{51}V+^{159}Tb reaction measurement was to learn more about the side-collision effect. However, it created interesting puzzles with no indication of it and the dominance of the αxn exit channel over the xn channel in the highly-excited region. It is very curious and interesting how these phenomena could be understood theoretically.

The authors would like to thank Tomasz Cap and the Warsaw group for their kind collaboration on theoretical model calculations. The present experiment was carried out in collaboration with the nSHE research group. We would like to thank the accelerator staff at the RIKEN Nishina Center (RNC) for providing a highly stable ^{51}V beam and for quickly changing the supplied beam energy throughout the beam time. We are grateful for the strong support of the RNC Director H. Sakurai.

REFERENCES

[1] H. Sakai *et al.*, *Eur. Phys. J. A* **58**, 238 (2022).

[2] M. Tanaka *et al.*, *J. Phys. Soc. Jpn.* **91**, (2022).

[3] P. Brionnet *et al.*, *RIKEN Accel. Prog. Rep.* **56**, 14 (2023).

[4] P. Brionnet *et al.*, *RIKEN Accel. Prog. Rep.* **56**, 16 (2023).

[5] K. Hagino *et al.*, *Comput. Phys. Commun.* **123**, 143 (1999).

[6] T. Cap, private communication.

[7] P. Möller *et al.*, *Phys. Rev. C* **91**, 024310 (2015).

[8] W.E. Parker *et al.*, *Phys. Rev. C* **44**, 774 (1991).

[9] J. Tōke, W.J. Świątecki, *Nucl. Phys. A* **372**, 141 (1981).

[10] For example, T. Cap, M. Kowal, K. Siwek-Wilczyńska, *Eur. Phys. J. A* **58**, 231 (2022).